JOURNAL OF GEOPHYSICAL RESEARCH, VOL. 86, NO. A1, PAGES 199-205, JANUARY 1, 1981

Auroral Plasma Lines: A First Comparison of Theory and Experiment

ELAINE S. ORAN,[1] VINCENT B. WICKWAR,[2] WLODEK KOFMAN,[3] AND ALICE NEWMAN[4]

In this preliminary report on low-energy (0.3 to 3 eV) secondary electrons in the auroral *E* layer (90 to 150 km), we compare intensities of plasma lines observed with the Chatanika radar to theoretical predictions obtained from a detailed numerical model. The model calculations are initiated with a flux of energetic auroral primary electrons which enter the atmosphere and lose energy to electrons, ions, and neutrals through a combination of elastic and inelastic collisions. This flux is chosen in order that the total calculated ionization rate matches one that is deduced from the radar measurements. From these same calculations the steady state secondary electron flux is deduced as a function of altitude, energy, and pitch angle. This flux is used to calculate plasma line intensities which are then compared with observed intensities. Initial comparisons suggest that the plasma line theory, when applied to low altitudes, must include the effect of electron-neutral collisions. When this is done, the good agreement obtained between theory and experiment indicates the promise of this approach for the study of low-energy auroral electrons.

1. INTRODUCTION

Enhancements of the intensity of plasma lines above the thermal level have been observed in the *F* region of the ionosphere at several incoherent scatter radar facilities [*Yngvesson and Perkins,* 1968; *Fremouw et al.,* 1969; *Evans and Gastman,* 1970; *Cicerone and Bowhill,* 1971; *Wickwar,* 1971; *Carlson et al.,* 1977; *Lejeune and Kofman,* 1977; *Oran et al.,* 1978; *Kofman and Lejeune,* 1980]. In these cases the suprathermal electrons responsible for the enhancements are local or conjugate photoelectrons created by solar ionization. Observations of plasma line spectra in the auroral *E* region have recently been made with the Chatanika incoherent scatter radar [*Wickwar,* 1978; *Kofman and Wickwar,* 1980]. In this case the suprathermal electrons are secondary electrons formed from the deposition of an incident flux of energetic electrons instead of photons. The radar's wavelength determines that the energies of the electrons that excite the plasma lines have phase energies ranging from a fraction of an electron volt to a few electron volts.

The previous lack of observational data on low-energy, low-altitude electrons has left unanswered many fundamental questions about their interactions and behavior. In the auroral region, some of these questions focus on the role of collisionless processes in determining the secondary electron spectra [*Papadopoulos and Coffey,* 1974; *Matthews et al.,* 1976; *Papadopoulos and Rowland,* 1978]. Uncertainties in the collision cross sections for low-energy electrons have arisen because of inconsistencies in the estimates of the energy required to heat thermal electrons to observed temperatures [*Carlson et al.,* 1977; *Kofman and Lejeune,* 1980]. Experimental and theoretical considerations have indicated that the modeling procedures and the cross sections in the energy range between thermal and suprathermal electrons are of questionable validity [*Kofman and Lejeune,* 1980; *Ashihara and Takyanagi,* 1974; *Jasperse,* 1976, 1977]. Finally, the large electron-neutral collision frequencies at low altitudes suggest that they must also be included in the basic calculation of plasma line intensities.

Detailed calculations and comparisons have proved very useful in studying plasma lines excited by photoelectrons. They have helped to define and resolve problems involving self-consistent calculations of electron temperatures [*Carlson et al.,* 1977], anisotropy in upshifted and downshifted plasma line intensities [*Oran et al.,* 1978], and the existence of large electron fluxes in the *F* region near the intersection of the thermal and photoelectron populations [*Kofman and Lejeune,* 1980].

This paper presents a first attempt to compare auroral *E* region observations to theoretical predictions. In the course of this paper we introduce the methodology for studying these questions. In the following section we present and describe the plasma line temperatures and the total ionization rates that have been derived from the radar measurements. We also discuss the accuracy of the effective recombination rate that must be used to determine the ionization rate. In section 3 we present the results of detailed model calculations of the plasma line temperatures. The calculations include determination of the secondary electron fluxes and the excitation and damping terms for the plasma lines. An important aspect of the plasma line portion of these calculations is the inclusion of a new term to describe the effects of electron-neutral collisions. We compare data and model calculations in section 4 and give our conclusions in section 5.

2. DATA DERIVED FROM THE RADAR MEASUREMENTS

Besides providing the plasma wave temperatures, the radar measurements also provide other data such as electron densities and exospheric temperatures that are used in our theoretical calculations. We are also able to deduce the total ion production rate which provides the normalization for the energetic auroral electron degradation calculation.

For the comparisons in this paper we have used data from two days: January 20, 1976, and March 19, 1978. Particular attention is paid to the March 19 data that have already been described, along with the radar and experimental procedures, by *Kofman and Wickwar* [1980]. On that date the auroral *E* layer was relatively stable and had a peak near 100 km. The data from January 20, 1976, which were obtained during the first Chatanika plasma line experiment [*Wickwar,* 1978], are included because the *E* layer peaked about 20 km higher. This

[1] Laboratory for Computational Physics, Naval Research Laboratory, Washington, D. C. 20375.

[2] Radio Physics Laboratory, SRI International, Menlo Park, California 94025. Present address: Division of Atmospheric Sciences, National Science Foundation, Washington, D. C. 20550.

[3] Centre d'Etude des Phénomènes Aléatoires et Géophysiques, BP 46, 38402 St. Martin d'Heres, France.

[4] JAYCOR, 205 South Whiting Street, Alexandria, Virginia 22304. Present address: Aerospace Corporation, El Segundo, California 90245.

Copyright © 1981 by the American Geophysical Union.

Paper number 80A0845.
0148-0227/81/080A-0845$01.00

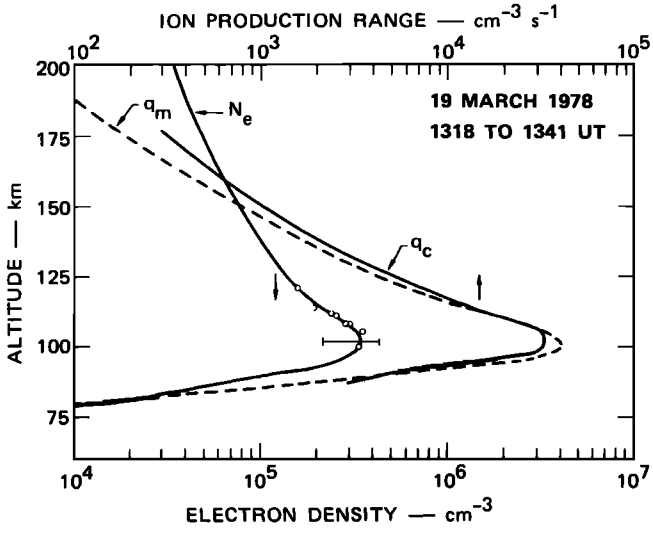

Fig. 1. Electron densities derived from ion (solid line) and plasma line (circles) components of the incoherent scatter spectrum for the period 1318–1341 UT (0318–0341 Alaskan Standard Time) on March 19, 1978. The bar at the peak of the layer shows the variation from 1-min integrations. The q_m curve of the ion production rate was obtained from the data by using (1) and (2). The q_c curve was obtained from the collisional, energetic electron deposition model.

altitude difference provides us with two very diverse situations to compare with our model, thereby strengthening our conclusions.

In Figure 1 we show the E region electron density profile for March 19, 1978 [*Kofman and Wickwar,* 1980]. The eight points on the solid curve were obtained from the frequency and altitude of the plasma lines measured with the filter bank. The altitude distribution of this signal allows the altitude of each point to be determined to within better than 2 km. The solid line is obtained from the total power in the ion component of the spectrum and has been appropriately corrected and scaled to fit the more accurate plasma line points.

The exospheric temperature is also needed for the neutral atmosphere model used in the detailed calculation. It has been calculated from ion temperatures near 300 km measured by the radar during periods without significant joule heating. In other experiments that had joule heating information available, we have found that the time scale for significant joule heating events and for the resultant ion temperature fluctuations was less than half an hour. Therefore we have taken periods during the experiment when the ion temperatures varied smoothly for longer than half an hour to indicate the lack of joule heating. Three to four hours before these plasma line measurements the exospheric temperature was 1000°K. By the time these data were taken, it may have risen to 1200°K. This possible range of variation has practically no effect on model neutral densities for our altitudes of prime interest (100 to 120 km) and very little effect even at altitudes at high as 150 km.

The total ion production rate in the E region, q_m, can be estimated from the electron density N_e when the effective recombination rate α_{eff} is known:

$$q_m = \alpha_{\text{eff}} N_e^2 \quad \text{cm}^{-3}\,\text{s}^{-1} \tag{1}$$

However, α_{eff} is a complex function of the ion composition and of the electron temperature. For moderate auroral conditions, the expression

$$\alpha_{\text{eff}} = 2.50 \times 10^{-6} \exp(-z/51.2)\ \text{cm}^3\,\text{s}^{-1} \tag{2}$$

where z is the altitude in kilometers has been shown to be a useful expression in comparing radar and photometer data [*Wickwar et al.,* 1975] and radar and satellite data [*Vondrak and Baron,* 1976]. Equations (1) and (2) together with the measured N_e profile give the q_m profile shown in Figure 1.

It is important to know how accurate this ion production rate profile is and in what regions of the ionosphere it is most accurate. In Figure 2 we compare α_{eff} from (2) to a profile determined experimentally by *Baron* [1974] from the decay of E region densities. Alternately, we can calculate α_{eff} for a mixture of NO^+ and O_2^+ ions:

$$\alpha_{\text{eff}} = \{\alpha_{NO^+}[NO^+] + \alpha_{O_2^+}[O_2^+]\}/N_e \quad \text{cm}^3\,\text{s}^{-1} \tag{3}$$

where we denote ion concentrations by square brackets and the total ion concentration is equal to the electron concentration N_e. For curve A in Figure 2 we assume that 67% of the ions are NO^+ and 33% are O_2^+. For curve B we assume that 90% of the ions are NO^+ and 10% are O_2^+. These two curves thus encompass a reasonable range of possible ratios of NO^+ and O_2^+ for the auroral E region [*Swider and Narcisi,* 1977].

To obtain these curves, we used the smooth electron temperature curve

$$T_e = 1715 - 1515 \exp[-0.01(z - 100)]\ \text{K} \tag{4}$$

shown in Figure 2 as a heavy dashed line. This temperature profile passes close to the radar-measured E region (three val-

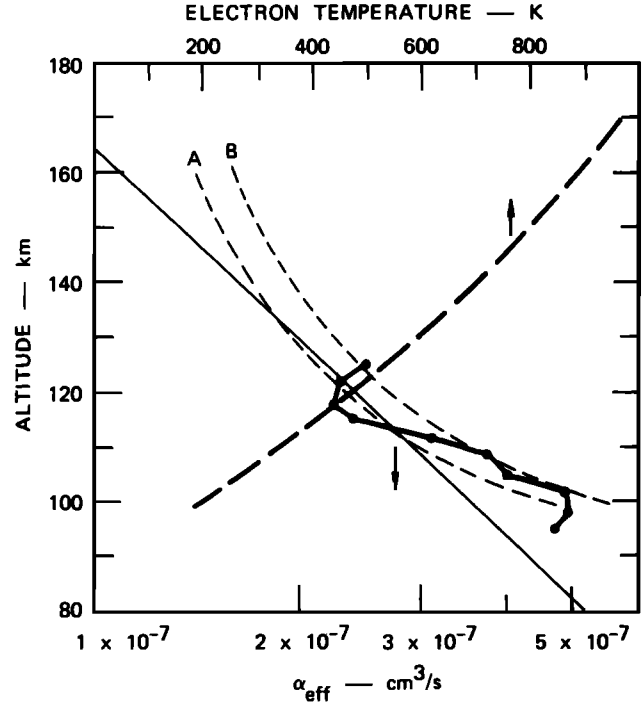

Fig. 2. Effective recombination rates and electron temperatures. The thin solid line is the α_{eff} from (2). The heavy solid line is the experimental α_{eff} for moderate auroral activity from *Baron* [1974]. The two dashed α_{eff} curves, A and B, result from the application of expressions for the recombination rates of NO^+ and O_2^+ [*Torr and Torr,* 1978] that are compatible with laboratory and satellite measurements, different mixtures of NO^+ and O_2^+, and electron temperatures. Curve A is for 67% NO^+ and 33% O_2^+. Curve B is for 90% NO^+ and 10% O_2^+. The heavy dashed curve is a smoothed representation of the measured electron temperatures for the period 1318–1341 UT on March 19, 1978 (equation (4)).

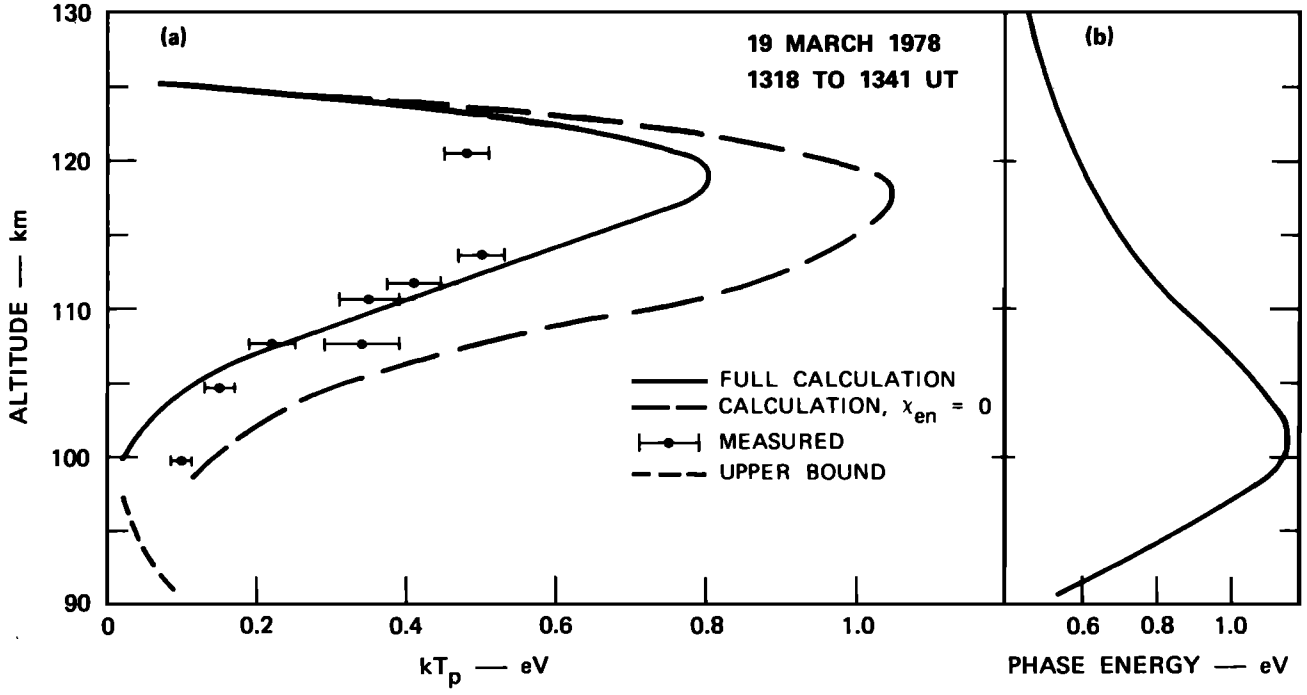

Fig. 3. (*a*) Plasma wave temperatures for 1318–1341 UT on March 19, 1978. The circles show the measured kT_p values in the topside of the *E* layer. The dashed curve in the bottomside shows the lower temperature limit for detecting plasma lines or an equivalent upper bound for the temperatures. The heavy dashed line shows the theoretically calculated kT_p values without electron-neutral collisions; the heavy solid line shows the temperatures with collisions. (*b*) Phase energies. The profile of phase energies for the plasma lines.

ues between 116 and 128 km) and *F* region (three values between 312 and 412 km) electron temperatures and passes through 200 K at 100 km. We then calculate α_{eff} by using the temperature-dependent recombination coefficients for both ions [*Torr and Torr,* 1978]:

$$\alpha_{NO^+} = 4.2 \times 10^{-7}\left(\frac{T_e}{300}\right)^{-0.85} \text{cm}^3\,\text{s}^{-1}$$
$$\alpha_{O_2^+} = 1.6 \times 10^{-7}\left(\frac{T_e}{300}\right)^{-0.55} \text{cm}^3\,\text{s}^{-1} \quad (5)$$

These coefficients are consistent with both laboratory measurements and model calculations fitted to Atmosphere Explorer satellite measurements.

Thus we see that those values of α_{eff} obtained by using the approximation given in (2) are within about 15% of what is obtained from either the experiment or from (3) between 110 km and 125 km, the altitude region most important for the plasma line comparisons. Similar good agreement between predictions of (2) and (3) extends at least another 10 km above the last experiment point, to 135 km. Above that, Figure 2 shows a slow divergence of α_{eff} values, but this does not affect our plasma line comparisons. This divergence would be less if there were a significant fraction of O^+ ions or if the electron temperature were greater. Below 110 km our estimate of q_m (employing (1) and (2)) may be too small by an amount that could be as much as 30% by 100 km.

The final important parameter that can be derived from the radar data is the plasma wave temperature kT_p. While the electron density is determined from the frequency of the plasma line signal, the plasma wave temperature is determined from the intensity of the signal and the range of altitudes from which it comes. The anlaysis procedure was first discussed by *Yngvesson and Perkins* [1968] and has been discussed in more detail for Chatanika data by *Wickwar* [1978] and *Kofman and Wickwar* [1980].

For the data from March 19, 1978, the plasma line intensity was measured by two methods: a filter bank and a high-speed correlator. The intensities have been compared and discussed by *Kofman and Wickwar* [1980]. Within the error bars the two sets of results are in agreement, and no difference exists between upshifted and downshifted plasma lines. Since the uncertainty is less for the filter bank data during this period, we used them to determine the plasma wave temperatures. In addition, the data presented in this paper are a combination of the upshifted and the downshifted data.

The other critical factor in the plasma wave temperature determination is the range extent of the scattering region. We may use either the ion component density profile or the range between the detected plasma lines. In both cases, we find values on the order of 1 km for our 100 kHz-wide filters.

The kT_p values were computed by two methods [*Kofman and Wickwar,* 1980] with the same results. The first method depends on the plasma line signal intensity and the absolute antenna gain; the second depends on the ratio of the plasma line signal intensity to ion component signal intensity. The resultant kT_p values are shown in Figure 3*a*. Also shown is a curve of the lower bound plasma wave temperatures that could have been detected with the filter bank. This curve thus provides an upper bound to the actual plasma line temperatures that would have been present below 100 km. All the detected plasma lines are from topside of the *E* layer.

The indicated error bars are the result of propagating the statistical uncertainty of the measured intensities. Possible systematic effects from spatial and temporal averaging are difficult to evaluate and have not been included. However, these effects are in opposite directions and to first order offset each

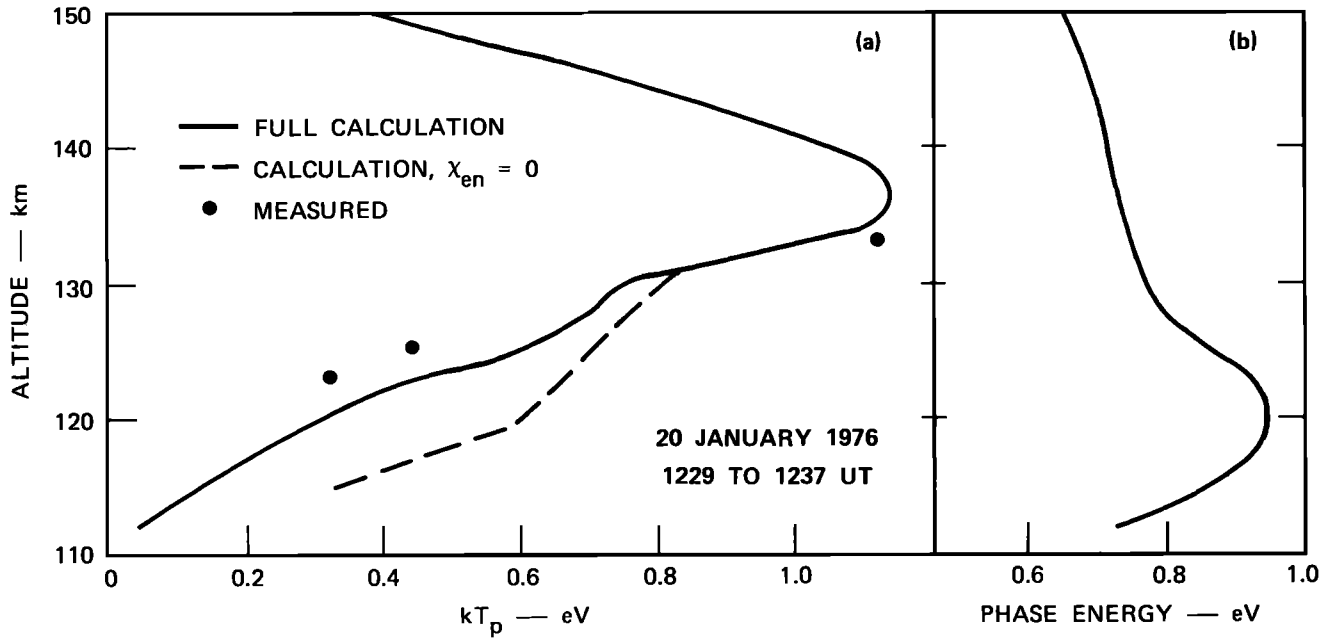

Fig. 4. (*a*) Plasma wave temperatures for 1229–1237 UT on January 20, 1976. The circles show the measured kT_p values. The heavy dashed line shows the theoretically calculated kT_p values without electron-neutral collisions; the heavy solid line shows the temperatures with collisions. (*b*) Phase energies. The profile of phase energies for the plasma lines.

other, with the possible exception of the point closest to the peak of the layer.

In Figure 3*b* we show the phase energy profile [*Yngvesson and Perkins,* 1968] determined from the electron densities. It indicates the minimum energy of the secondary electrons that interact with the plasma waves.

The experimental procedure on January 20, 1976, was similar to that used for March 19, 1978, but was less comprehensive, since no *E* region temperatures were measured and the filter bank had only three filters [*Wickwar,* 1978]. The plasma wave temperatures for January 20 are given in Figure 4*a*, and the phase energy profile in Figure 4*b*.

3. Model Calculation

In order to find the secondary electron flux required to calculate plasma wave temperatures we used the energetic electron deposition model developed by *Strickland et al.* [1976] that is based on a finite difference solution of the collisional Boltzmann equation. This model has been shown to be accurate for suprathermal electrons created by either the solar EUV or for auroral electrons [*Oran and Strickland,* 1978]. The model requires the specification of an incident or local spectrum of primary energetic electrons, an ambient electron density profile, and a neutral atmosphere model. The principal output is the degraded electron flux $\varphi(z, \mu, E)$, where z is the altitude, μ is the pitch angle, and E is the energy. Important by-products of the calculation include the total production rate of ions, the production rates of excited and ionized species, and the heat loss to the thermal electrons.

Most of the input quantities have already been discussed in the previous section. The *Jacchia* [1971] neutral model was used with an exospheric temperature of 1000°K. We chose an appropriate incident energetic electron flux by iterating on an initial guess until the resultant total ionization rates agreed with those obtained with the radar over the altitude range of the plasma line observations. Any discrepancies between the two ionization profiles outside this limited altitude range are assumed to be of lesser importance to the plasma line calculation, which depends only on local variables. The calculated profile q_c is shown in Figure 1. In fact, good agreement between profiles was achieved over the full altitude range. The resultant incident electron fluxes for the two days are shown in Figure 5.

The numerical aspects of the electron deposition calculations have been checked by reducing the size of the energy and altitude meshes, varying the altitude of the boundary conditions, and testing for energy conservation. Convergence tests of this type have been reported previously [*Strickland et al.,* 1976; *Oran and Strickland,* 1976, 1978].

Also important are tests of the sensitivity of the derived fluxes to the input parameters. Initial tests which varied the neutral temperature and species densities by as much as 30% caused negligible changes in the derived fluxes at the *E* region altitudes of interest. More detailed tests of these input data will be performed as part of the extensive comparison between the data and model planned for a later date.

Typical secondary electron fluxes are shown in Figure 6 for altitudes between about 90 and 150 km and between 0.3 and 10 eV. These calculated fluxes show the same general behavior as those measured by *Sharp and Hays* [1974]. There is a dip at about 2.5 eV due to absorption in the vibrational bands of N_2 and a bump at about 4 eV. These general features have also been calculated by *Rees et al.* [1969]. It is primarily the flux between 100 and 120 km and 0.3 and 2.0 eV that is important for these plasma line observations.

The plasma line temperatures are then calculated from these secondary electron fluxes using the method described by *Oran et al.* [1978]. For this we are required to use the same electron density and neutral model as in the flux calculation.

The calculation of the plasma wave temperature kT_p is based on

$$\frac{kT_p}{kT_e} = \frac{f_p + f_m + \chi_{ei} + \chi_{en}}{L_p + f_m + \chi_{ei} + \chi_{en}} \quad (6)$$

where the terms in the numerator and denominator of the right-hand side describe the excitation and damping of plasma waves. The function f_m is the contribution of the thermal electrons to the excitation and Landau damping of the plasma waves [*Yngvesson and Perkins,* 1968]. The functions f_p and L_p are the contribution of suprathermal electrons (photoelectrons or secondary electrons) to the excitation and Landau damping, respectively, of the plasma waves. They have been treated in detail by *Fremouw et al.* [1969] and *Oran et al.* [1978]. In the absence of a magnetic field or when the direction of the radar beam is along the magnetic field, both f_p and L_p simplify to functions involving the one-dimensional velocity distribution [*Yngvesson and Perkins,* 1968]. As a consistency check on the form of f_p and L_p, we note that if the velocity distribution of the suprathermal electrons were Maxwellian, f_p and L_p would reduce to the form of f_m. The function χ_{ei} represents the excitation and damping of plasma waves due to electron-ion collisions [*Yngvesson and Perkins,* 1968] and is proportional to the electron-ion collision frequency [*Wickwar,* 1971; *Oran et al.,* 1978]. The function χ_{en} is a similar term that we introduce to account for the excitation and damping due to electron-neutral collisions.

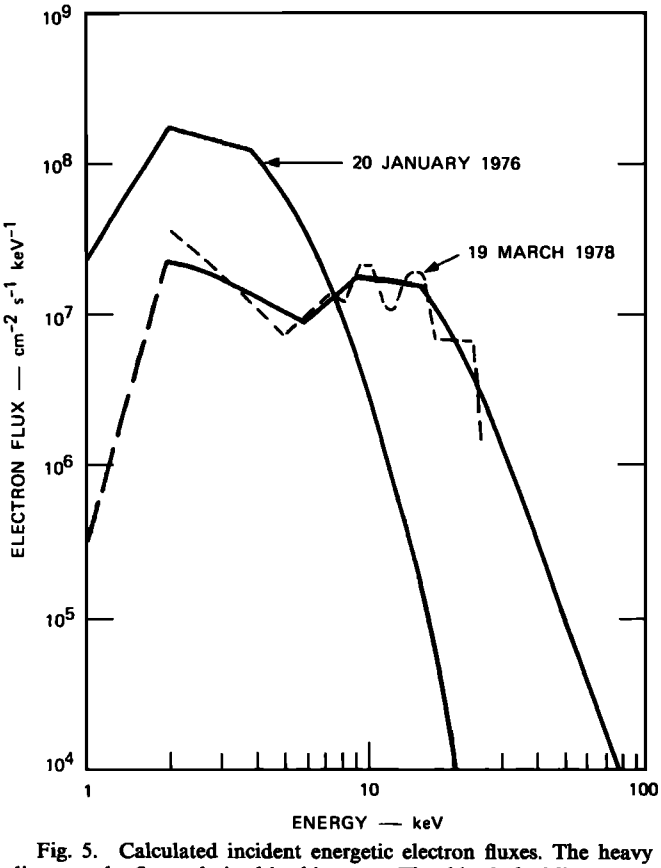

Fig. 5. Calculated incident energetic electron fluxes. The heavy lines are the fluxes derived in this paper. The thin dashed line corresponds to the result of using the UNTANGLE code [*Vondrak and Baron,* 1976].

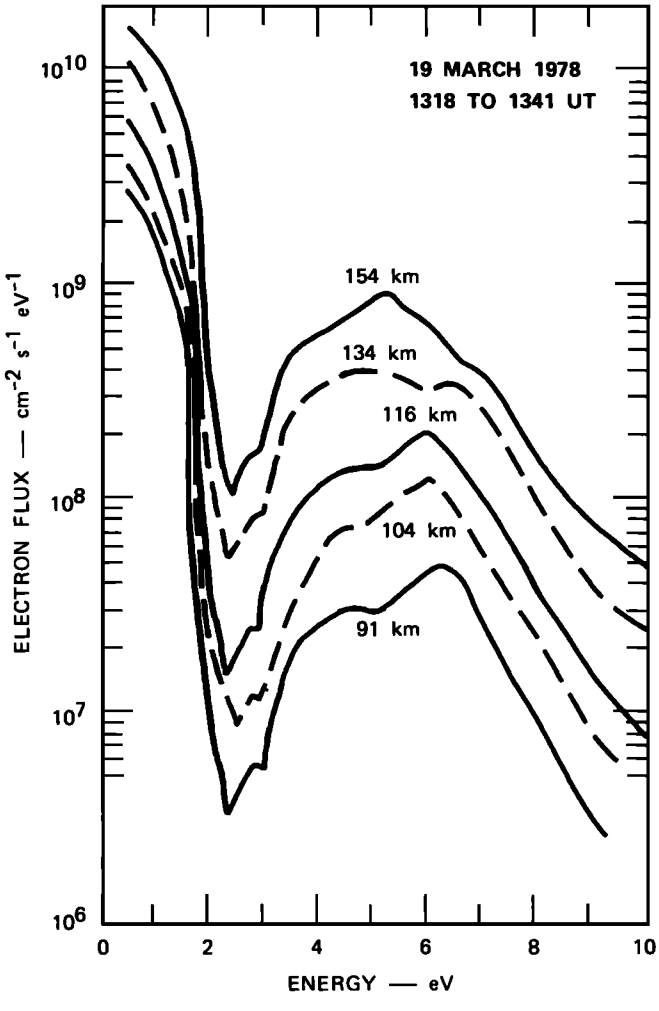

Fig. 6. Calculated secondary electron fluxes in the auroral *E* layer for March 19, 1978.

The electron temperatures used in (6) are those obtained from a steady state calculation that uses the same neutral atmosphere model and electron density data as in the electron deposition calculation. The heat source term is equal to the term for energy loss by secondary electrons to ambient electrons in the $\varphi(E, \mu, z)$ calculation. This part of the calculation will be extended and refined in a future paper in order to obtain better estimates of T_e which may be compared to data.

The new contribution to (6) is the inclusion of the effects of electron-neutral collisions, which become important at low altitudes. Recently, *Newman and Oran* [1981] calculated the contribution of electron-neutral collisions χ_{en} by applying fluctuation dissipation theory and Salpeter's approximation to the collisional Boltzmann equation. For the parameter range of interest, the BGK collision term may be represented as the sum of the electron-neutral collision frequency (including both elastic and inelastic contributions from dominant neutral species [*Oran et al.,* 1974]) and a suitably defined electron-ion Coulomb collision frequency. They found χ_{en} to be proportional to the electron-neutral collision frequency with the same constant of proportionality as in the electron-ion collision term χ_{ei}.

For the data from March 19, 1978, the terms of (6) are shown individually in Figure 7 as a function of altitude. The

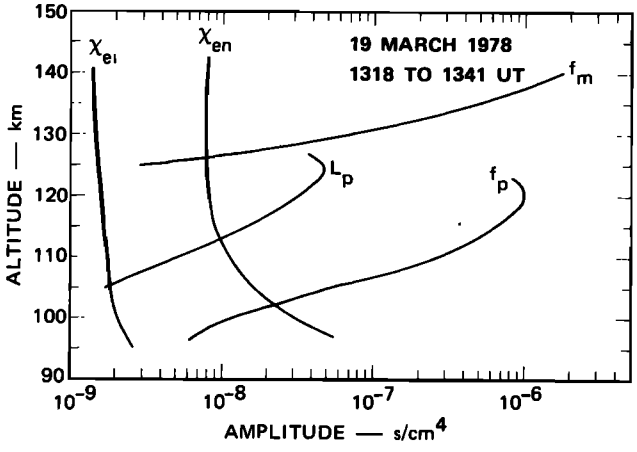

Fig. 7. Calculated excitation and damping terms for the plasma wave temperatures for March 19, 1978.

calculated plasma wave temperatures are shown in Figure 3*a*, both with and without electron-neutral collisions. Similar plasma wave temperature calculations performed for the data from January 20, 1976, are shown in Figure 4*a*.

4. Comparison of Observations and Calculations

In Figures 3 and 4 we see that below 130 km there is a significant difference between the two sets of model calculations depending upon whether or not electron-neutral collisions are included in the plasma line portion of the calculations. Most importantly, we see that the experimental values are in good agreement with the calculated values that include collisions.

Still more information can be obtained from the comparison of model calculation and experiment by examining the contribution of each term in (6). These terms are shown individually in Figure 7 for the calculation of plasma wave temperatures for March 19, 1978. In the altitude region between 105 and 115 km, there is very good agreement between theory and experiment. In this region the f_p term from the secondary electrons and the χ_{en} term from electron-neutral collisions dominate. Hence the good agreement supports our detailed calculations of both of these terms. Below 100 km the χ_{en} term alone dominates. The agreement with the upper bound for the experimental temperatures is significant support for the calculation of this term. As indicated previously, model calculations would be most affected for altitudes near 100 km by the possible systematic errors in the estimate of α_{eff}. Hence disagreement at that altitude is not considered to be significant.

At higher altitudes, between 115 and about 120 km, the f_p and L_p terms dominate. Because of the coupling between them, agreement in this region would be more indicative of the shape than the magnitude of the velocity distribution. Above about 125 km the f_m term from the ambient electrons dominates. Comparisons in this region provide information mostly about T_e. The disagreement between calculation and experiment at 121 km could indicate that the f_p term was too small or, more likely, that the calculated T_e and f_m were too small. Because of the strong dependence of f_m on T_e, a much smaller error in T_e than in the secondary electron flux would be required to produce this discrepancy. Previous findings [*Carlson et al.*, 1977; *Kofman and Lejeune*, 1980] also suggest that our model calculations may somewhat underestimate T_e.

The model calculations reproduce other features of kT_p profiles that have appeared in the observations. The calculations predict that plasma lines on the bottomside of the E layer are too small to be detected; in fact, they are not observed. The maximum kT_p value in the calculated profile occurs at an altitude above the peak of the E layer and hence at a plasma frequency well below the maximum frequency. This theoretical result is consistent with the observations reported here and by *Kofman and Wickwar* [1980]. Another predicted feature is the rapid decrease in kT_p with height above the altitude of the maximum value. This is consistent with the data presented by *Wickwar* [1978] and *Kofman and Wickwar* [1980]. The decrease, as discussed by *Wickwar* [1978] and verified by the theoretical calculations presented here, is due to the increasing influence of thermal electrons as a function of increasing altitude.

5. Conclusion

This first comparison of observations and theoretical model calculations for plasma lines at Chatanika shows that we are able to extend the analysis of plasma lines to the auroral E layer. The calculations start from a flux of energetic auroral electrons that is adjusted to obtain the electron-ion production rates determined from the radar measurements. The fluxes of secondary electrons determined by the collisional electron deposition model are then combined with the plasma line theory to obtain plasma wave temperatures that are compared to the observations.

As discussed in section 4, there is good agreement between the results of the calculations and observations when we extend the plasma line theory by introducing a term for electron-neutral collisions. For this term it has been shown [*Newman and Oran*, 1981] that a form analogous to that of the term for electron-ion collisions is required. While this is the principal damping term in the lower E region, it would have no effect on previous calculations made for higher altitudes.

The auroral E layer data discussed in this paper have provided the first opportunity to test the viability of theoretical model calculations at low suprathermal electron energies. The good agreement between model calculations and experimental results strongly supports the physical models adopted for calculating the secondary electron flux and all of the elastic and inelastic cross sections used. Because the model does well and no collisionless effects are included, we conclude that collisionless effects are not significant within this low-altitude, low-energy range.

In the future we plan to do more extensive comparisons of observed and calculated plasma lines in the auroral E layer at Chatanika. In doing so we will not only increase the variety of geophysical conditions that can affect the relative importance of different terms in the calculations, but we will further constrain the calculations by extending the comparisons to measurements of electron temperatures and auroral emissions. There are also available considerable daytime plasma line data from the E and F regions at Chatanika which will enable us to examine the transition region between thermal electrons and photoelectrons. Comparisons of this type should also be made with data from the European incoherent scatter radar. There, the use of both the UHF and VHF frequencies would enable a much wider range of phase energies to be examined.

Acknowledgments. The authors would like to acknowledge the help of P. Palmadesso, R. McCann, and D. Strickland for consultation on the calculational portion of this work, which was funded by

the Naval Research Laboratory through the Office of Naval Research. The French portion of the experiment was supported by the Actions Thématiques Programmées of the Centre National de la Recherche Scientifique for the International Magnetospheric Study. It was supported, as well, by the Centre de Recherches en Physique de l'Environnement Terrestre et Planetaire and by the Centre National d'Etudes des Télécommunications. The American portion of the experimental work was supported by grant ATM78-00129 from the Aeronomy Program, Division of Atmospheric Sciences, National Science Foundation. In addition, the Chatanika radar was operated by SRI International under contract DNA001-77-C-0042 from the Defense Nuclear Agency and grant ATM72-01644-A05 from the Division of Atmospheric Sciences, National Science Foundation.

The Editor thanks H. Carlson for his assistance in evaluating this report.

REFERENCES

Ashihara, O., and K. Takyanagi, Velocity distribution of ionospheric low-energy electrons, *Planet. Space Sci., 22,* 1201–1217, 1974.

Baron, M. J., Electron densities within aurorae and other auroral *E*-region characteristics, *Radio Sci., 9,* 341–348, 1974.

Carlson, H. C., V. B. Wickwar, and G. P. Mantas, The plasma line revisited as an aeronomical diagnostic: Suprathermal electrons, solar EUV, electron-gas thermal balance, *Geophys. Res. Lett., 4,* 565–567, 1977.

Cicerone, R. J., and S. A. Bowhill, Photoelectron fluxes measured at Millstone Hill, *Radio Sci., 6,* 957–966, 1971.

Evans, J. V., and I. J. Gastman, Detection of conjugate photoelectrons at Millstone Hill, *J. Geophys. Res., 75,* 807–815, 1970.

Fremouw, E. J., J. Petriceks, and F. W. Perkins, Thomson scatter measurements of magnetic field effects of the Landau damping and excitation of plasma waves, *Phys. Fluids, 12,* 869–874, 1969.

Jacchia, L. G., Revised static models of the thermosphere and exosphere with empirical temperature profiles, *Spec. Rep. 332,* Smithson. Astrophys. Observ., Cambridge, Mass., 1971.

Jasperse, J. R., Boltzmann-Fokker-Planck model for the electron distribution function in the earth's ionosphere, *Planet. Space Sci., 24,* 33–40, 1976.

Jasperse, J. R., Electron distribution function and ion concentrations in the earth's lower ionosphere from Boltzmann-Fokker-Planck theory, *Planet. Space Sci., 25,* 743–756, 1977.

Kofman, W., and G. Lejeune, Determination of low energy photoelectron distribution from plasma line measurements at Saint Santin, *Planet. Space Sci., 28,* 1980.

Kofman, W., and V. Wickwar, Plasma line measurements at Chatanika with high-speed correlator and filter bank, *J. Geophys. Res., 85,* 2998–3012, 1980.

Lejeune, G., and W. Kofman, Photoelectron distribution determination from plasma line intensity measurements obtained at Nancay (France), *Planet. Space Sci., 25,* 123–133, 1977.

Matthews, D. L., M. Pongratz, and K. Papadopoulos, Nonlinear production of suprathermal tails in auroral electrons, *J. Geophys. Res., 81,* 123–129, 1976.

Newman, A., and E. S. Oran, The effects of electron-neutral collisions on the intensity of plasma lines, *J. Geophys. Res., 86,* in press, 1981.

Oran, E. S., and D. J. Strickland, Calculation of the ionospheric photoelectron distribution function, *Memo. Rep. 3361,* Nav. Res. Lab., Washington, D. C., 1976.

Oran, E. S., and D. J. Strickland, Photoelectron flux in the earth's ionosphere, *Planet. Space Sci., 26,* 1161–1177, 1978.

Oran, E. S., T. R. Young, Jr., D. V. Anderson, T. P. Coffey, P. C. Kepple, A. W. Ali, and D. F. Strobel, A numerical model of the mid-latitude ionosphere, *Memo. Rep. 2839,* Nav. Res. Lab., Washington, D. C., 1974.

Oran, E. S., P. J. Palmadesso, and S. Ganguly, Low-altitude plasma line anisotropy, *J. Geophys. Res., 83,* 2190–2194, 1978.

Papadopoulos, K., and T. Coffey, Anomalous resistivity in the auroral plasma, *J. Geophys. Res., 79,* 1558–1561, 1974.

Papadopoulos, K., and H. L. Rowland, Collisionless effects on the spectrum of secondary auroral electrons at low altitudes, *J. Geophys. Res., 83,* 5768–5772, 1978.

Rees, M. H., A. I. Stewart, and J. C. G. Walker, Secondary electrons in aurora, *Planet. Space Sci., 17,* 1997–2008, 1969.

Sharp, W. E., and P. B. Hays, Low-energy auroral electrons, *J. Geophys. Res., 79,* 4319–4321, 1974.

Strickland, D. J., D. L. Book, T. P. Coffey, and J. A. Fedder, Transport equation techniques for the deposition of auroral electrons, *J. Geophys. Res., 81,* 2755–2764, 1976.

Swider, W., and R. S. Narcisi, Auroral *E*-region: Ion composition and nitric oxide, *Planet. Space Sci., 25,* 103–116, 1977.

Torr, D. G., and M. R. Torr, Review of rate coefficients of ionic reactions determined from measurements made by the Atmosphere Explorer satellites, *Rev. Geophys. Space Phys., 16,* 327–340, 1978.

Vondrak, R. R., and M. J. Baron, Radar measurements of the latitudinal variations of auroral ionization, *Radio Sci., 11,* 939–946, 1976.

Wickwar, V. B., Photoelectrons from the magnetic conjugate point studied by means of the 6300A predawn enhancement and the plasma line enhancement, Ph.D. thesis, Rice Univ., Houston, Tex., 1971.

Wickwar, V. B., Plasma lines in the auroral *E* layer, *J. Geophys. Res., 83,* 5186–5190, 1978.

Wickwar, V. B., M. J. Baron, and R. D. Sears, Auroral energy input from energetic electrons and joule heating at Chatanika, *J. Geophys. Res., 80,* 4364–4367, 1975.

Yngvesson, K. O., and F. W. Perkins, Radar Thomson scatter studies of photoelectrons in the ionosphere and Landau damping, *J. Geophys. Res., 73,* 97–110, 1968.

(Received February 26, 1980;
revised May 19, 1980;
accepted May 19, 1980.)